Isogeometric Analysis

Thomas J.R. Hughes* and John A. Evans

Abstract

We present an introduction to Isogeometric Analysis, a new methodology for solving partial differential equations (PDEs) based on a synthesis of Computer Aided Design (CAD) and Finite Element Analysis (FEA) technologies. A prime motivation for the development of Isogeometric Analysis is to simplify the process of building detailed analysis models for complex engineering systems from CAD representations, a major bottleneck in the overall engineering process. However, we also show that Isogeometric Analysis is a powerful methodology for providing more accurate solutions of PDEs, and we summarize recently obtained mathematical results and describe open problems.

1. Introduction

Designers generate CAD (Computer Aided Design) files and these must be translated into analysis-suitable geometries, meshed and input to large-scale finite element analysis (FEA) codes. This task is far from trivial and for complex engineering designs is now estimated to take over 80% of the overall analysis time, and engineering designs are becoming increasingly more complex; see Figure 1. For example, presently, a typical automobile consists of about 3,000 parts, a fighter jet over 30,000, the Boeing 777 over 100,000, and a modern nuclear submarine over 1,000,000. Engineering design and analysis are not separate endeavors. Design of sophisticated engineering systems is based on a wide range of computational analysis and simulation methods, such as structural mechanics, fluid dynamics, acoustics, electromagnetics, heat transfer, etc. Design speaks to analysis, and analysis speaks to design. However, analysis-suitable models

---

*Institute for Computational Engineering and Sciences, University of Texas at Austin, 1 University Station, Austin, Texas 78735, U.S.A. E-mail: hughes@ices.utexas.edu
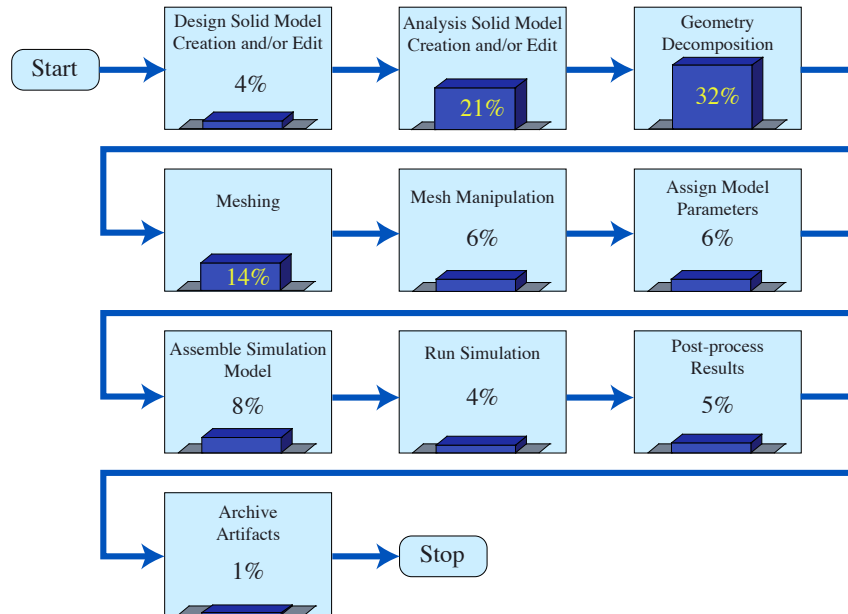
Figure 1. Engineering designs are becoming increasingly complex, making analysis a time consuming and expensive endeavor. (Courtesy of General Dynamics / Electric Boat Division.)

are not automatically created or readily meshed from CAD geometry. Although not always appreciated in the academic analysis community, model generation is much more involved than simply generating a mesh. There are many time consuming, preparatory steps involved. And one mesh is no longer enough. According to Steve Gordon, Principal Engineer, General Dynamics Electric Boat Corporation, "We find that today's bottleneck in CAD-CAE integration is not only automated mesh generation, it lies with efficient creation of appropriate 'simulation-specific' geometry." (In the commercial sector analysis is usually referred to as CAE, which stands for Computer Aided Engineering.) The anatomy of the process has been studied by Ted Blacker, Manager of Simulation Sciences, Sandia National Laboratories. At Sandia, mesh generation accounts for about 20% of overall analysis time, whereas creation of the analysis-suitable geometry requires about 60%, and only 20% of overall time is actually devoted to analysis per se; see Figure 2. The 80/20 modeling/analysis ratio seems to be a very common industrial experience, and there is a strong desire to reverse it, but so far little progress has been made, despite enormous effort to do so. The integration of CAD and FEA has proven a formidable problem. It seems that fundamental changes must take place to fully integrate engineering design and analysis processes.

It is apparent that the way to break down the barriers between engineering design and analysis is to reconstitute the entire process, but at the same
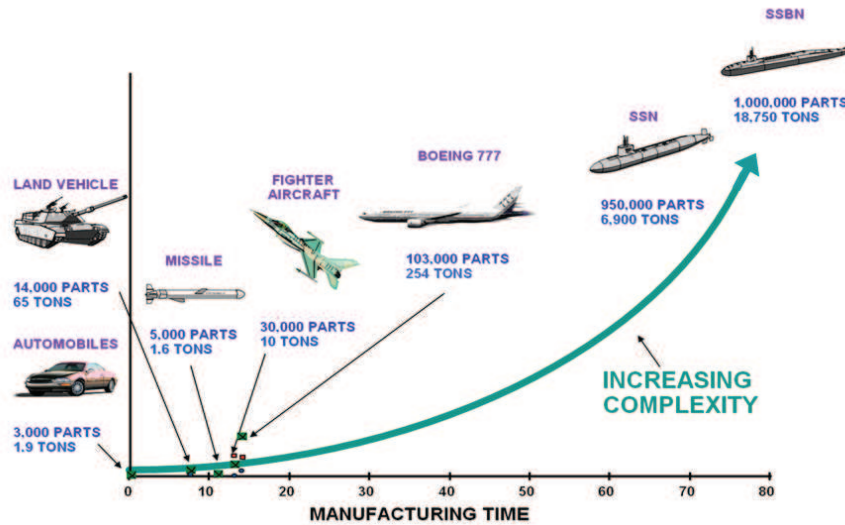
Figure 2. Estimation of the relative time costs of each component of the model generation and analysis process at Sandia National Laboratories. Note that the process of building the model completely dominates the time spent performing analysis. (Courtesy of Michael Hardwick and Robert Clay, Sandia National Laboratories.)

time maintain compatibility with existing practices. A fundamental step is to focus on one, and only one, geometric model, which can be utilized directly as an analysis model, or from which geometrically precise analysis models can be automatically built. This will require a change from classical FEA to an analysis procedure based on CAD representations. This concept is referred to as **Isogeometric Analysis**, and it was introduced in [21]. Since then a number of additional papers have appeared [1, 2, 3, 5, 6, 7, 8, 9, 13, 14, 16, 18, 19] as well as a book [12].

There are a number of candidate computational geometry technologies that may be used in Isogeometric Analysis. The most widely used in engineering design are NURBS (non-uniform rational B-splines), the industry standard (see [17, 22, 23, 11]). The major strengths of NURBS are that they are convenient for free-form surface modeling, can exactly represent all conic sections, and therefore circles, cylinders, spheres, ellipsoids, etc., and that there exist many efficient and numerically stable algorithms to generate NURBS objects. They also possess useful mathematical properties, such as the ability to be refined through knot insertion, C^{p-1}-continuity for pth-order NURBS, and the variation diminishing and convex hull properties. NURBS are ubiquitous in CAD systems, representing billions of dollars in development investment. One may argue the merits of NURBS versus other computational geometry technologies, but their preeminence in engineering design is indisputable. As such, they were the natural starting point for Isogeometric Analysis and their use in an analysis setting is the focus of this paper.

T-splines [24, 25] are a recently developed forward and backward generalization of NURBS technology. T-splines extend NURBS to permit local refinement and coarsening, and are very robust in their ability to efficiently sew together adjacent patches. Commercial T-spline plug-ins have been introduced in Maya and Rhino, two NURBS-based design systems (see references [27] and [28]). Initiatory investigations of T-splines in an Isogeometric Analysis context have been undertaken by [4] and [15]. These works point to a promising future for T-splines as an isogeometric technology.

2. Basics of NURBS-based Isogeometric Analysis

In FEA there is one notion of a mesh and one notion of an element, but an element has two representations, one in the parent domain and one in the physical space. Elements are usually defined by their nodal coordinates and the degrees-of-freedom are usually the values of the basis functions at the nodes. Finite element basis functions are typically interpolatory and may take on positive and negative values. Finite element basis functions are often referred to as "interpolation functions," or "shape functions." See [20] for a discussion of the basic concepts.

In NURBS, the basis functions are usually not interpolatory. There are two notions of meshes, the control mesh[1] and the physical mesh. The control points define the control mesh, and the control mesh interpolates the control points. The control mesh consists of multilinear elements, in two dimensions they are bilinear quadrilateral elements, and in three dimensions they are trilinear hexahedra. The control mesh does not conform to the actual geometry. Rather, it is like a scaffold that controls the geometry. The control mesh has the look of a typical finite element mesh of multilinear elements. The control variables are the degrees-of-freedom and they are located at the control points. They may be thought of as "generalized coordinates." Control elements may be degenerated to more primitive shapes, such as triangles and tetrahedra. The control mesh may also be severely distorted and even inverted to an extent, while at the same time, for sufficiently smooth NURBS, the physical geometry may still remain valid (in contrast with finite elements).

The physical mesh is a decomposition of the actual geometry. There are two notions of elements in the physical mesh, the patch and the knot span. The patch may be thought of as a macro-element or subdomain. Most geometries utilized for academic test cases can be modeled with a single patch. Each patch has two representations, one in a parent domain and one in physical space.

---

[1]The control mesh is also known as the "control net," the "control lattice," and curiously the "control polygon" in the univariate case.
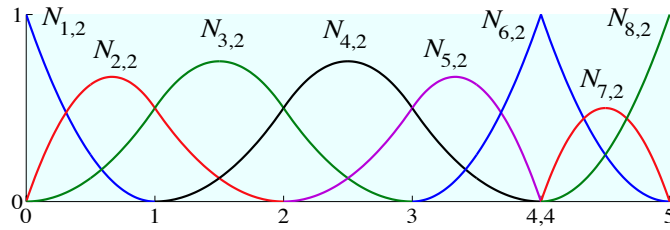
Figure 3. Quadratic B-spline basis functions for open, non-uniform knot vector $\Xi = \{0, 0, 0, 1, 2, 3, 4, 4, 5, 5, 5\}$.

In two-dimensional topologies, a patch is a rectangle in the parent domain representation. In three dimensions it is a cuboid.

Each patch can be decomposed into knot spans. Knots are points, lines, and surfaces in one-, two-, and three-dimensional topologies, respectively. Knot spans are bounded by knots. These define element domains where basis functions are smooth (*i.e.*, C^∞). Across knots, basis functions will be C^{p-m} where p is the degree[2] of the polynomial and m is the multiplicity of the knot in question. Knot spans are convenient for numerical quadrature. They may be thought of as micro-elements because they are the smallest entities we deal with. They also have representations in both a parent domain and physical space. When we speak of "elements" without further description, we usually mean knot spans.

There is one other very important notion that is a key to understanding NURBS, the **index space** of a patch. It uniquely identifies each knot and discriminates among knots having multiplicity greater than one.

NURBS basis functions are the rational counterpart of standard B-spline basis functions. For a discussion of the construction of B-spline basis functions on the parent domain from preassigned knot vectors, see Chapter 2 of [12]. A quadratic example is presented in Figure 3. B-spline basis functions exhibit many desirable properties, including partition of unity, compact support, and point-wise positivity. Multi-dimensional basis functions are defined through a tensor product, and basis functions are defined in physical space through a **push-forward**, *i.e.* by considering a composition with the inverse of the geometrical mapping. In Isogeometric Analysis, the **isoparametric** concept is invoked. That is, the same basis is used for both geometry and analysis. Analogues of h- and p-refinement also exist in Isogeometric Analysis in the form of knot insertion and order elevation, and there is a new refinement scheme called k-refinement. See Chapter 2.1.4 of [12].

---

[2]There is a terminology conflict between the geometry and analysis communities. Geometers will say a cubic polynomial has degree 3 and order 4. In geometry, order equals degree plus one. Analysts will say a cubic polynomial is order three, and use the terms order and degree synonymously. This is the convention we adhere to.

See Table 2 for a summary of NURBS paraphernalia employed in Isogeometric Analysis. A schematic illustration of the ideas is presented in Figure 4 for a NURBS surface in $\mathbb{R}^3$. For more details on B-splines and NURBS, see [17, 22, 23, 11].

Index Space		
Control Mesh	Physical Mesh	
Multilinear Control Elements	Patches	Knot Spans
Topology: **1D:** Straight lines defined by two consecutive control points	Patches: Images of rectangular meshes in the parent domain mapped into the actual geometry. Patches may be thought of as macro-elements or subdomains.	Topology of knots in the parent domain: **1D:** Points **2D:** Lines **3D:** Planes
2D: Bilinear quadrilaterals defined by four control points	Topology: **1D:** Curves **2D:** Surfaces **3D:** Volumes	Topology of knots in the physical space: **1D:** Points **2D:** Curves **3D:** Surfaces
3D: Trilinear hexahedra defined by eight control points	Patches are decomposed into knot spans, the smallest notion of an element.	Topology of knots spans, *i.e.*, "elements": **1D:** Curved segments connecting consecutive knots **2D:** Curved quadrilaterals bounded by four curves **3D:** Curved hexahedra bounded by six curved surfaces

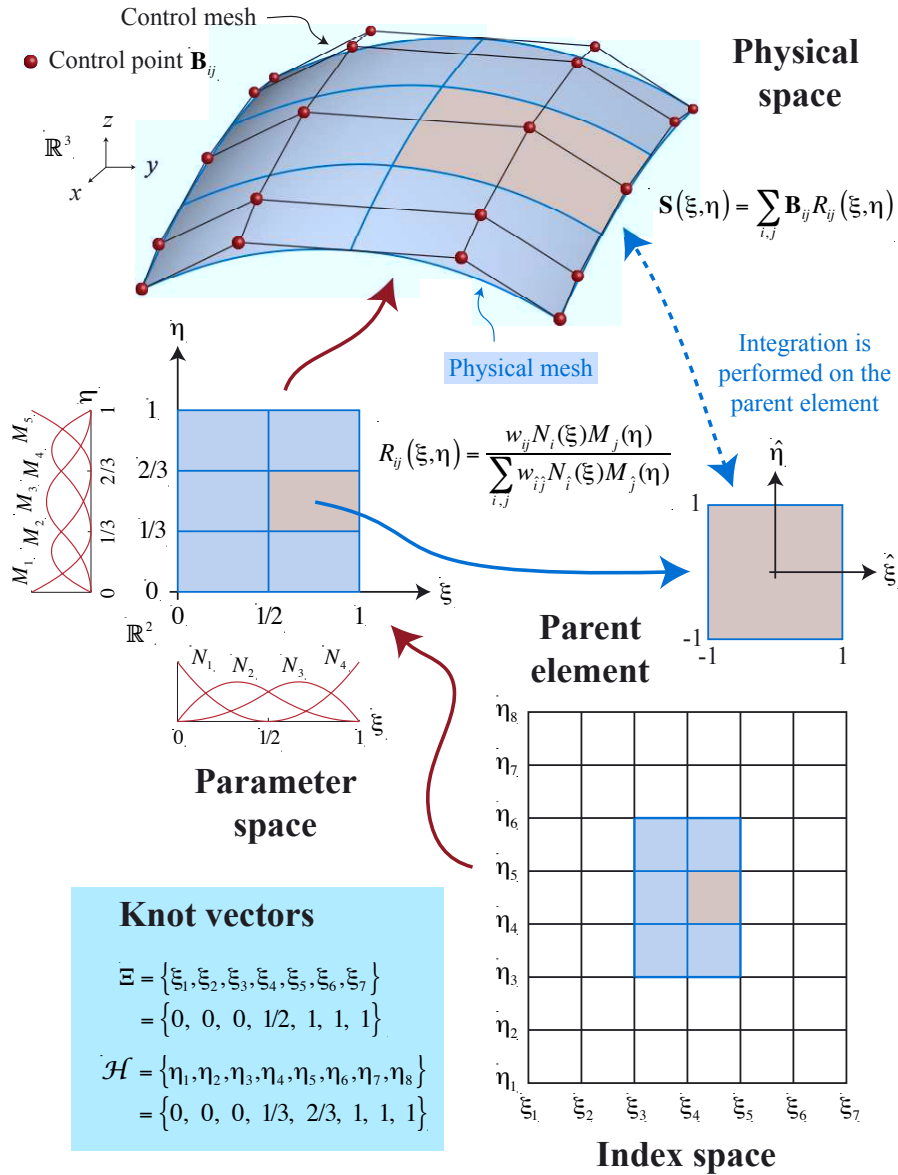Table 1. NURBS paraphernalia in Isogeometric Analysis

Figure 4. Schematic illustration of NURBS paraphernalia for a one-patch surface model. Open knot vectors and quadratic C^1-continuous basis functions are used. Complex multi-patch geometries may be constructed by assembling control meshes as in standard FEA. Also depicted are C^1-quadratic ($p = 2$) basis functions determined by the knot vectors. Basis functions are multiplied by control points and summed to construct geometrical objects, in this case a surface in $\mathbb{R}^3$. The procedure used to define basis functions from knot vectors is described in detail in Chapter 2 of [12].

3. Boundary Value Problems

As an example of solving a differential equation posed over the domain defined by a NURBS geometry, let us consider Laplace's equation. The goal is to find $u : \bar{\Omega} \to \mathbb{R}$ such that

$$\Delta u + f = 0 \quad \text{in} \quad \Omega, \tag{1a}$$

$$u = g \quad \text{on} \quad \Gamma_D, \tag{1b}$$

$$\nabla u \cdot \mathbf{n} = h \quad \text{on} \quad \Gamma_N, \tag{1c}$$

$$\beta u + \nabla u \cdot \mathbf{n} = r \quad \text{on} \quad \Gamma_R, \tag{1d}$$

where $\overline{\Gamma_D \bigcup \Gamma_N \bigcup \Gamma_R} = \Gamma \equiv \partial\Omega$, $\Gamma_D \bigcap \Gamma_N \bigcap \Gamma_R = \varnothing$, and $\mathbf{n}$ is the unit outward normal vector $\partial\Omega$. The functions $f : \Omega \to \mathbb{R}$, $g : \Gamma_D \to \mathbb{R}$, $h : \Gamma_N \to \mathbb{R}$, and $r : \Gamma_R \to \mathbb{R}$ are all given, as is the constant β. Equation (1) constitutes the **strong form** of the boundary value problem (BVP). The boundary conditions given in (1b), (1c), and (1d) represent the three major types of boundary conditions one is likely to encounter. These are Dirichlet conditions, Neumann conditions, and Robin conditions, respectively.

For a sufficiently smooth domain, and under certain restrictions on g, h, and r, a unique solution u satisfying (1) is known to exist, but an analytical expression will usually be impossible to obtain. However, we may seek an approximate solution of the form

$$u^h = \sum_A d_A N_A \tag{2}$$

where N_A is a basis function and d_A is an unknown to be determined. We generically refer to techniques for doing so as **numerical methods**. Different numerical methods are simply different techniques for finding d_A such that $u^h \approx u$. We focus here on the Bubnov-Galerkin method that underlies most of modern FEA.

The technique begins by defining a weak, or variational, counterpart of (1). To do so, we need to characterize two classes of functions. The first is to be composed of candidate, or trial solutions. From the outset, these functions will be required to satisfy the Dirichlet boundary condition of (1b).

To define the trial and weighting spaces formally, let us first define the space of square integrable functions on Ω. This space, called $L^2(\Omega)$, is defined as the collection of all functions $u : \Omega \to \mathbb{R}$ such that

$$\int_\Omega u^2 \, d\Omega < +\infty. \tag{3}$$

Let us consider a multi-index $\boldsymbol{\alpha} \in \mathbb{N}^d$ where d is the number of spatial dimensions in the space. For $\boldsymbol{\alpha} = \{\alpha_1, \ldots, \alpha_d\}$, we define $|\boldsymbol{\alpha}| = \sum_{i=1}^d \alpha_i$. We now have a concise way to represent derivative operators. Let $D^{\boldsymbol{\alpha}} = D_1^{\alpha_1} D_2^{\alpha_2} \ldots D_d^{\alpha_d}$, where $D_i^j = \frac{\partial^j}{\partial x_i^j}$. So that certain expressions to be employed in the formulation

make sense, we shall require that the derivatives of the trial solutions be square-integrable. Such a function is said to be in the Sobolev space $H^1(\Omega)$, which is characterized by

$$H^1(\Omega) = \{u | D^{\boldsymbol{\alpha}} u \in L^2(\Omega), |\boldsymbol{\alpha}| \leq 1\}. \tag{4}$$

We may now define the collection of **trial solutions**, denoted by $\mathcal{S}$, as all of the function which have square-integrable derivatives and that also satisfy

$$u|_{\Gamma_D} = g. \tag{5}$$

This is written as

$$\mathcal{S} = \{u \mid u \in H^1(\Omega), u|_{\Gamma_D} = g\}. \tag{6}$$

The second collection of functions in which we are interested is called the **weighting functions**. This collection is very similar to the trial functions, except that we have the homogeneous counterpart of the Dirichlet boundary condition. That is, the weighting functions are denoted by a set $\mathcal{V}$ defined by

$$\mathcal{V} = \{w \mid w \in H^1(\Omega), w|_{\Gamma_D} = 0\}. \tag{7}$$

We may now obtain a variational statement of the BVP by multiplying (1a) by an arbitrary test function $w \in \mathcal{V}$ and integrating by parts, incorporating (1c) and (1d) as needed. The resulting weak form of the problem is now: Given f, g, h, and r, find $u \in \mathcal{S}$ such that for all $w \in \mathcal{V}$

$$\int_\Omega \nabla w \cdot \nabla u \, d\Omega + \beta \int_{\Gamma_R} wu \, d\Gamma$$
$$= \int_\Omega wf \, d\Omega + \int_{\Gamma_N} wh \, d\Gamma + \int_{\Gamma_R} wr \, d\Gamma. \tag{8}$$

This weak form may be rewritten as

$$a(w, u) = L(w) \tag{9}$$

where

$$a(w, u) = \int_\Omega \nabla w \cdot \nabla u \, d\Omega + \beta \int_{\Gamma_R} wu \, d\Gamma, \tag{10}$$

and

$$L(w) = \int_\Omega wf \, d\Omega + \int_{\Gamma_N} wh \, d\Gamma + \int_{\Gamma_R} wr \, d\Gamma. \tag{11}$$

This concise notation, or variants thereof, is quite common in the finite element literature. For problems other than the Laplace equation, the details vary, but the basic form remains. It captures the essential mathematical features of the variational method (as well as suggesting features of a finite element implementation) that are more general than the details of the equation itself.

The solution to (8), or equivalently (9), is called a **weak solution**. Under appropriate regularity assumptions, it can be shown that the weak solution and the strong solution of (1) are equivalent; see [20].

The Bubnov-Galerkin method, abbreviated as Galerkin's method, consists of constructing finite-dimensional approximations of $\mathcal{S}$ and $\mathcal{V}$, denoted $\mathcal{S}^h$ and $\mathcal{V}^h$, respectively. Strictly speaking, these will be subsets such that

$$\mathcal{S}^h \quad \subset \quad \mathcal{S}, \tag{12}$$

$$\mathcal{V}^h \quad \subset \quad \mathcal{V}. \tag{13}$$

Furthermore, these will be associated with subsets of the space spanned by the isoparametric basis. In Isogeometric Analysis, these spaces consist of mapped NURBS functions.

We can further characterize $\mathcal{S}^h$ by recognizing that if we have a *given* function $g^h \in \mathcal{S}^h$ such that $g^h|_{\Gamma_D} = g$, then for every $u^h \in \mathcal{S}^h$, there exists a unique $v^h \in \mathcal{V}^h$ such that

$$u^h = v^h + g^h. \tag{14}$$

We can now write a variational equation of the form of (9). The Galerkin form of the problem is: Given g^h, h, and r, find $u^h = v^h + g^h$, where $v^h \in \mathcal{V}^h$, such that for all w^h in $\mathcal{V}^h$

$$a(w^h, u^h) = L(w^h). \tag{15}$$

Recalling (14) and the bilinearity of $a(\cdot, \cdot)$, we can rewrite (15) as

$$a(w^h, v^h) = L(w^h) - a(w^h, g^h). \tag{16}$$

In this latter form, the unknown information is on the left-hand-side, while everything on the right-hand-side is given, as before.

The finite-dimensional nature of the function spaces used in Galerkin's method leads to a coupled system of linear algebraic equations. Let the solution space consist of all linear combinations of a given set of NURBS functions $N_A : \hat{\Omega} \to \mathbb{R}$, where $A = 1, \ldots, n_{np}$. Without loss of generality, we may assume a numbering for these functions such that there exists an integer $n_{eq} < n_{np}$ such that

$$N_A|_{\Gamma_D} = 0 \quad \forall A = 1, \ldots, n_{eq}. \tag{17}$$

Thus, for all $w^h \in \mathcal{V}^h$, there exist constants c_A, $A = 1, \ldots, n_{eq}$ such that

$$w^h = \sum_{A=1}^{n_{eq}} N_A c_A. \tag{18}$$

Furthermore, the function g^h (frequently called a "lifting") is given similarly by coefficients g_A, $A = 1, \ldots, n_{np}$. In practice, we will always choose g^h such that $g_1 = \ldots = g_{n_{eq}} = 0$ as they have no effect on its value on Γ_D, and so

$$g^h = \sum_{A=n_{eq}+1}^{n_{np}} N_A g_A. \tag{19}$$

Finally, recalling again (14), for any $u^h \in \mathcal{S}^h$ there exist d_A, $A = 1, \ldots, n_{eq}$ such that

$$u^h = \sum_{A=1}^{n_{eq}} N_A d_A + \sum_{B=n_{eq}+1}^{n_{np}} N_B g_B = \sum_{A=1}^{n_{eq}} N_A d_A + g^h. \tag{20}$$

Proceeding to define

$$
\begin{aligned}
K_{AB} &= a(N_A, N_B), & (21) \\
F_A &= L(N_A) - a(N_A, g^h), & (22)
\end{aligned}
$$

and

$$
\begin{aligned}
\mathbf{K} &= [K_{AB}], & (23) \\
\mathbf{F} &= \{F_A\}, & (24) \\
\mathbf{d} &= \{d_A\}, & (25)
\end{aligned}
$$

for $A, B = 1 \ldots, n_{eq}$, we can rewrite (16) as the matrix problem

$$\mathbf{Kd} = \mathbf{F}. \tag{26}$$

The matrix $\mathbf{K}$ is commonly referred to as the stiffness matrix, and $\mathbf{F}$ and $\mathbf{d}$ are referred to as the force and displacement vectors, respectively.

It is important to note that $\mathbf{K}$ is a sparse matrix. This is a result of the fact that the support of each basis function is highly localized. Thus, for many combinations of A and B in the $n_{eq} \times n_{eq}$ global stiffness matrix, $K_{AB} = a(N_A, N_B) = 0$. We can take advantage of this fact in order to reduce the amount of work necessary in building and solving the algebraic system. Things are further simplified by employing Gaussian quadrature to perform integrations. This process is detailed in Section 3.3.1 of [12]. Even though the NURBS functions are not necessarily polynomials, Gaussian quadrature seems to be very effective for integrating them. Though this approach to integration is only approximate, it is important to note that integrating the classical polynomial functions by quadrature on elements with curved sides is only an approximation as well.

Once Galerkin's method has been applied and an approximation, u^h, has been obtained, it is fair to inquire as to just how good of an approximation it is. Results for classical FEA and Isogeometric Analysis are discussed in the next session. It turns out that, for elliptic problems such as the one considered in this section, the solution is optimal in a very natural sense; see Chapter 4 of [20].

4. Error Estimates for NURBS

4.1. FEA. Well established *a priori* approximation results exist for classical finite elements applied to elliptic problems (see, for example, the classic text

by [10]). The Sobolev space of order r is defined by

$$H^r(\Omega) = \{\mathbf{u} | D^{\boldsymbol{\alpha}} \mathbf{u} \in L^2(\Omega), |\boldsymbol{\alpha}| \le r\}. \tag{27}$$

The norm associated with $H^r(\Omega)$ is given by

$$\|\mathbf{u}\|_r^2 = \sum_{|\boldsymbol{\alpha}| \le r} \int_\Omega (D^{\boldsymbol{\alpha}} \mathbf{u}) \cdot (D^{\boldsymbol{\alpha}} \mathbf{u}) \, d\mathbf{x}. \tag{28}$$

In classical FEA, the fundamental error estimate for the elliptic boundary value problem, expressed as a bound on the difference between the exact solution, $\mathbf{u}$, and the FEA solution, $\mathbf{u}^h$, takes the form

$$\|\mathbf{u} - \mathbf{u}^h\|_m \le Ch^\beta \|\mathbf{u}\|_r, \tag{29}$$

where $\| \cdot \|_m$ and $\| \cdot \|_r$ are the norms corresponding to Sobolev spaces $H^m(\Omega)$ and $H^r(\Omega)$, respectively, h is a characteristic length scale related to the size of the elements in the mesh, $\beta = \min(p+1-m, r-m)$ where p is the polynomial order of the basis, and C is a constant that does not depend on $\mathbf{u}$ or h.

The term of interest in (29) is h^β. The mesh parameter, h, can be defined in several ways, with the specific definition affecting C. A fairly general definition is the diameter of the smallest circle (in two dimensions) or sphere (in three dimensions) that is large enough to circumscribe any element in the mesh. The ***order of convergence***, β, expresses how the error changes under refinement of the mesh. In particular, if we use h-refinement to bisect each of the elements in the mesh (*i.e.*, h is replaced with $h/2$), we would expect the error to decrease by a factor of $(1/2)^\beta$.

4.2. NURBS. The extremely technical details of the process of obtaining a result analogous to (29) for NURBS can be found in [3]. Here we present the basic ideas, but encourage the interested reader to consult the original publication.

For classical FEA polynomials, the result in (29) is obtained by first establishing the interpolation properties of the basis. Let Π_m be the projection operator from $H^m(\Omega)$ into the space spanned by the FEA basis. Then the optimal interpolate is the function

$$\eta^h = \Pi_m u \tag{30}$$

such that

$$\|u - \eta^h\|_m \le \|u - v^h\|_m \quad \forall v^h \in \mathcal{S}^h, \tag{31}$$

where $\mathcal{S}^h$ is the finite element space. To establish just how good this optimal approximation is (*i.e.*, to determine how can $\|u - \eta^h\|_m$ be bounded), we obtain a bound on each element, and then sum over all of the elements to get a global result. With this interpolation result in hand, the second step in the process is

to relate the result of the Galerkin finite element method, u^h, to the optimal interpolate, η^h. In particular, it can be shown that the order of convergence of the finite element solution is the same as for the optimal interpolate. Taken together, these two results yield the the bound (29), which states that (up to a constant) Galerkin's method gives us the optimal result.

When we seek an analogous result for NURBS, we face several difficulties. The first is that the approximation properties of this rational basis are harder to determine than are those of a standard polynomial basis. In particular, note that the weights are determined by the geometry and so are out of our control when we attempt to approximate a field over that geometry and cannot be adjusted to improve the result. The second difficulty originates from the large support of the spline functions. Standard interpolation estimates seek to find a best fit within each element and then aggregate these results to obtain an approximation over the entire domain. This is non-trivial with the spline functions because the support of each function spans several elements, and so we cannot determine optimal values for the control variables by looking at each element individually. The issue is further complicated by the possibility of differing levels of continuity (and thus differing sizes of the the supports of the functions) throughout the domain.

To overcome the fact that the basis is rational rather than polynomial, we first note that the parameter space $\hat{\Omega}$ can be considered to be the unit cube $[0, 1]^d$. No generality is lost in this assumption as dividing a knot vector by a constant or adding a constant does not change the resulting physical domain in any way. Let us first denote a NURBS basis function as:
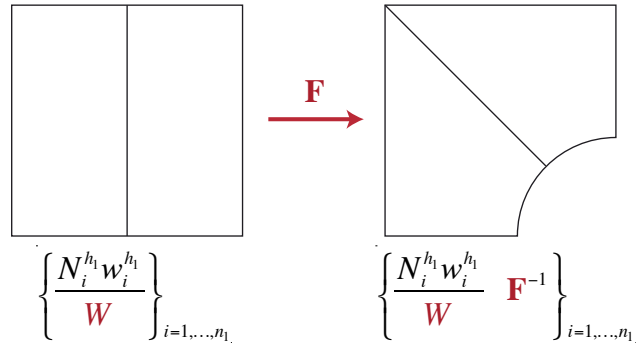
$$R_i(\xi) = \frac{N_i(\xi)w_i}{W(\xi)}, \tag{32}$$

with

$$W(\xi) = \sum_{i=1}^{n} N_i(\xi)w_i \tag{33}$$

where N_i is the corresponding B-spline basis function. The important thing to note is that the weighting function[3], $W(\xi)$, does not change as we h-refine the mesh (it does not change under p-refinement either, though this is not the case we are interested in at present). While both the weights and the basis functions change, they do so in such a way as to leave $W(\xi)$ unaltered. Similarly, the geometrical mapping from the parameter space into the physical space, $\mathbf{F} : \hat{\Omega} \to \Omega$, does not change as we insert new knot values. See Figure 5. It remains exactly the same at all levels of refinement. To take advantage of this fact, we consider the function we wish to approximate, $u : \Omega \to \mathbb{R}^\ell$. As the geometrical mapping is one-to-one, we can pull this back to the parametric

---

[3]Do not confuse this use of the term "weighting function" with the unrelated use of the same terminology in Galerkin's method.

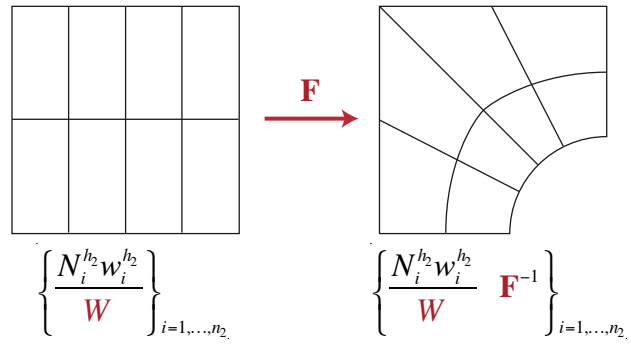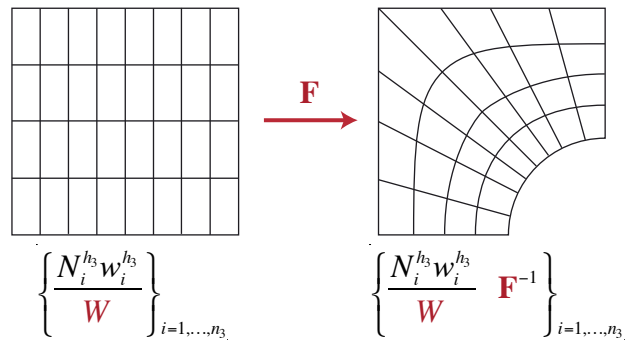$$\left\{ \frac{N_i^{h_1} w_i^{h_1}}{W} \right\}_{i=1,\ldots,n_1}$$

$$\left\{ \frac{N_i^{h_1} w_i^{h_1}}{W} \ \mathbf{F}^{-1} \right\}_{i=1,\ldots,n_1}$$

(a) Coarse mesh

$$\left\{ \frac{N_i^{h_2} w_i^{h_2}}{W} \right\}_{i=1,\ldots,n_2}$$

$$\left\{ \frac{N_i^{h_2} w_i^{h_2}}{W} \ \mathbf{F}^{-1} \right\}_{i=1,\ldots,n_2}$$

(b) First h-refinement

$$\left\{ \frac{N_i^{h_3} w_i^{h_3}}{W} \right\}_{i=1,\ldots,n_3}$$

$$\left\{ \frac{N_i^{h_3} w_i^{h_3}}{W} \ \mathbf{F}^{-1} \right\}_{i=1,\ldots,n_3}$$

(c) Second h-refinement

Figure 5. As we h-refine the mesh, the basis functions N_i and weights w_i change, but the geometrical mapping $\mathbf{F}$ and the weighting function W are *completely fixed* at the coarsest level of discretization. They do not change under refinement.

domain to define $\hat{u} = u \circ \mathbf{F}^{-1} : \hat{\Omega} \rightarrow \mathbb{R}^\ell$. Lastly, we can lift the image of the function using the weighting function to define $\tilde{u} = \{W\hat{u}, W\} : \hat{\Omega} \rightarrow \mathbb{R}^{\ell+1}$. Recalling that we obtain the rational basis in $\mathbb{R}^d$ by a projective transformation (equivalent to dividing by W) of a B-spline basis in $\mathbb{R}^{d+1}$, we see that the ability of the rational NURBS basis to approximate u on Ω is intimately related to the ability of the underlying B-spline basis to approximate $\tilde{u}$ on $\hat{\Omega}$. Thus we have reduced the problem of understanding a rational basis on a general domain to that of understanding a polynomial basis on the unit cube.

The second hurdle is more technical. The fact that each function has support over many elements and that the continuity across the various element boundaries can vary from one boundary to the next greatly complicates matters compared with the classical case. [3] address this difficulty by proving approximation results in so-called "bent" Sobolev spaces in which the continuity varies throughout the domain. A sequence of lemmas is established leading up to an approximation result that includes not only the norm in these bent Sobolev spaces of the function u being approximated, but also the gradient of the mapping, $\nabla\mathbf{F}$. This last term presents no problem because, as already discussed, it does not change as the mesh is refined, and thus does not affect the rate of convergence. The resulting approximation result is: Let k and l be integer indices such that $0 \leq k \leq l \leq p+1$, and let $u \in H^l(\Omega)$; then

$$\sum_{e=1}^{n_{el}} |u - \Pi_k u|_{H^k(\Omega^e)}^2 \leq C \sum_{e=1}^{n_{el}} h_e^{2(l-k)} \sum_{i=0}^{l} \|\nabla\mathbf{F}\|_{L^\infty(\mathbf{F}^{-1}(\Omega^e))}^{2(i-l)} |u|_{H^i(\Omega^e)}^2. \qquad (34)$$

The constant C depends on p and the shape (but not size) of the domain Ω, as well as the shape regularity of the mesh. The factors involving the gradient of the mapping render the estimate dimensionally consistent.

Finally, with the approximation result of (34) in hand, establishing the manner in which the Isogeometric Analysis solution, u^h, relates to the optimal interpolate, η^h, proceeds exactly as in the classical case. Combining these results yields the desired result: *The Isogeometric Analysis solution obtained using NURBS of order p has the same order of convergence as we would expect in a classical FEA setting using classical basis functions with a polynomial order of p.* This is an exceptionally strong result as it is independent of the order of continuity that the mesh possesses. That is, bisecting all of the elements in an FEA mesh (thus cutting the mesh parameter from h to $h/2$) requires the introduction of many more degrees-of-freedom than does bisection of the same number of NURBS elements while maintaining $p-1$ continuity (see Section 2.1.4 of [12]). This means that NURBS can converge at the same rate as FEA polynomials, while remaining much more efficient.

4.3. Explicit *h-k-p*-estimates for NURBS.
The theoretical study of [3] is continued in [6], focusing on the relation between the degree p and the global regularity k of a NURBS space and its approximation properties. Indeed, error estimates that are explicit in terms of the mesh-size h, and p, k are

obtained. The approach is restricted to C^{k-1} approximations, with $2k - 1 \leq p$. The interesting case of higher regularity, up to $k = p$, is still open. However, the results give an indication of the role of the smoothness k and offer a first mathematical justification of the potential of Isogeometric Analysis based on globally smooth NURBS. The main result, in a simplified form and in the two-dimensional setting, is the following: let v be a function to be approximated. Then there exists a NURBS approximation Πv such that

$$|v - \Pi v|_{H^\ell(\Omega_e)} \leq C(p - k + 1)^{-(\sigma-\ell)} h_e^{\sigma-\ell} \|v\|_{H^\sigma(\Omega_e)} \tag{35}$$

where Ω_e is a mesh element of diameter h_e in the NURBS physical domain Ω, $2k \leq \sigma \leq p + 1$, and $\ell \leq k$. In [6], different asymptotic regimes are studied. In particular, when v is smooth, the strong advantage of higher k is shown.

5. Vibrations

The study of structural vibrations or, more specifically, of eigenvalue problems allows us to examine in more detail the approximation properties of the smooth NURBS functions independently of any geometrical considerations. In general, **spectrum analysis** is the term applied to the study of how numerically computed natural frequencies, ω_n^h, compare with the analytically computed natural frequencies, ω_n. We will see that, for a given number of degrees-of-freedom and bandwidth, the use of NURBS results in dramatically improved accuracy in spectral calculations over classical FEA.

Let us begin by considering one of the simplest vibrational model problems in one dimension: the longitudinal vibrations of an elastic rod. If we consider the domain $\Omega = (0, L) \subset \mathbb{R}$, there is no longer an issue of geometrical accuracy. FEA basis functions and NURBS[4] are equally capable of representing this domain exactly, and so the quality of the results will depend entirely on the approximation properties of the basis.

To understand the formulation of the eigenproblem representing the longitudinal vibrations of a "fixed-fixed" elastic rod, let us begin by considering the elastodynamics equation from which it is derived. The behavior of the rod, which is assumed to move only in the longitudinal direction, is governed by the equations of linear elasticity combined with Newton's second law, resulting in

$$(Eu_{,x})_{,x} - \rho u_{,tt} = 0 \quad \text{in} \quad \Omega \times (0, T), \tag{36a}$$

$$u = 0 \quad \text{on} \quad \Gamma \times (0, T), \tag{36b}$$

where $\Omega = (0, L)$, $\rho : (0, L) \to \mathbb{R}$ is the density per unit length of the rod, $E : (0, L) \to \mathbb{R}$ is Young's modulus, and the "fixed-fixed" condition (36b)

---

[4]In this simple domain, the NURBS reduce to the special case of B-splines.

ensures that the ends of the rod do not move. For an actual dynamics problem, we would need to augment (36) with appropriate initial conditions of the form

$$
\begin{align}
u(x,0) &= u_0(x), \tag{37} \\
u_{,t}(x,0) &= v_0(x). \tag{38}
\end{align}
$$

At present, however, we are not interested in the transient behavior of the rod. Instead, we are interested in the natural frequencies and modes in which the rod vibrates. We obtain these by separation of variables. In a slight abuse of notation, we assume $u(x,t)$ to have the form

$$
u(x,t) = u(x)e^{i\omega t}, \tag{39}
$$

where $u(x)$ is a function of only the spatial variable, x, while $i = \sqrt{-1}$, and ω is the natural frequency. Inserting (39) into (36a) and dividing by the common exponential term results in the eigenproblem we are seeking:

$$
\begin{align}
(Eu_{,x})_{,x} + \omega^2 \rho u = 0 &\quad \text{in} \quad \Omega, \tag{40a} \\
u = 0 &\quad \text{on} \quad \Gamma. \tag{40b}
\end{align}
$$

Equation (40) constitutes an eigenproblem for the rod. The nontrivial solutions are countably infinite. That is, for $k = 1, 2, \ldots, \infty$, there is an eigenvalue $\lambda_k = (\omega_k)^2$ and corresponding eigenfunction $u_{(k)}$ satisfying (40). Furthermore, $0 < \lambda_1 \leq \lambda_2 \leq \ldots$, and the eigenfunctions are orthogonal. Though the eigenfunctions are only defined up to a multiplicative constant, we can remove the arbitrariness by augmenting the orthogonality condition to include normality.

Following the now familiar process, we multiply (40a) by a test function w and integrate by parts to obtain the weak form of the equation: Find all eigenpairs $\{u, \lambda\}$, $u \in \mathcal{S}$, $\lambda = \omega^2 \in \mathbb{R}^+$, such that for all $w \in \mathcal{V}$

$$
a(w,u) - \omega^2 (w, \rho u) = 0, \tag{41}
$$

where

$$
a(w,u) = \int_0^L w_{,x} E u_{,x} \, dx, \tag{42}
$$

$$
(w, \rho u) = \int_0^L w \rho u \, dx. \tag{43}
$$

Note that, due to the homogeneous boundary conditions, $\mathcal{S} = \mathcal{V} = H_0^1(0,L) = \{u \in H^1(0,L) | u(0) = u(L) = 0\}$.

The Galerkin formulation is obtained by restricting ourselves to finite-dimensional subspaces $\mathcal{S}^h \subset \mathcal{S}$ in the usual way. That is, w and u in (41)

will be replaced by finite dimensional approximations w^h and u^h of the form

$$w^h = \sum_{A=1}^{n_{eq}} N_A d_A \quad \text{and} \quad u^h = \sum_{B=1}^{n_{eq}} N_B c_B, \tag{44}$$

respectively. The resulting eigenpairs will contain approximations of both natural modes $u_{(k)}^h$ and the natural frequencies ω_k^h. The problem becomes: Find all $\omega^h \in \mathbb{R}^+$ and $u^h \in \mathcal{S}^h$ such that for all $w^h \in \mathcal{V}^h$

$$a(w^h, u^h) - (\omega^h)^2 (w^h, \rho u^h) = 0. \tag{45}$$

Substituting the shape-function expansions for w^h and u^h in (45) gives rise to a matrix eigenvalue problem: Find natural frequency $\omega_k^h \in \mathbb{R}^+$ and eigenvector $\boldsymbol{\Psi}_k$, $k = 1, \ldots, n_{eq}$, such that

$$\left(\mathbf{K} - (\omega_k^h)^2 \mathbf{M} \right) \boldsymbol{\Psi}_k = \mathbf{0}, \tag{46}$$

where

$$\mathbf{K} = [K_{AB}], \tag{47}$$
$$\mathbf{M} = [M_{AB}], \tag{48}$$

with

$$K_{AB} = a(N_A, N_B), \tag{49}$$
$$M_{AB} = (N_A, \rho N_B), \tag{50}$$

and $\boldsymbol{\Psi}_k$ is the vector of control variables corresponding to $u_{(k)}^h$.

As before, we refer to $\mathbf{K}$ as the ***stiffness matrix***. The new object, $\mathbf{M}$, is the ***mass matrix***. Noting that $\rho > 0$, and that the NURBS basis functions are pointwise non-negative, we see from (43) that every entry in the mass matrix is also non-negative. This claim cannot be made for standard finite elements.

Let us consider the case where ρ, E, and L are each taken to be 1. Analytically, (40a) can be solved to obtain $\omega_n = n\pi$ for $n = 1, \ldots, \infty$. We can assess the quality of the numerical method by comparing the ratio of the computed modes, ω_n^h, with the analytical result. That is, $(\omega_n^h/\omega_n) = 1$ indicates that the numerical frequency is identical to the analytical result. In practice, the discrete frequencies will always obey the relationship

$$\omega_n \leq \omega_n^h \quad \text{for} \quad n = 1, \ldots, n_{eq}, \tag{51}$$

and so we expect the ratio (ω_n^h/ω_n) to be greater than 1 (see, *e.g.*, [26]), with larger values indicating decreased accuracy.

Figure 6 shows a comparison of k-method (C^{p-1} pth-order NURBS) and p-method (C^0 pth-order finite elements) numerical spectra for $p = 1, \ldots, 4$ (we recall that for $p = 1$ the two methods coincide). Here, the superiority of the isogeometric approach is evident, as one can see that for C^0 finite elements the higher modes *diverge* with p. This negative result shows that even higher-order
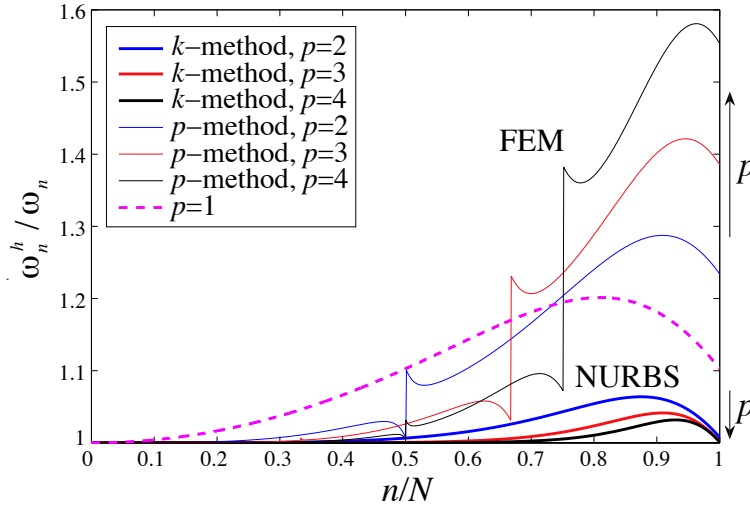
Figure 6. Longitudinal vibrations of an elastic rod. Comparison of k-method and p-method numerical spectra.

finite elements have no approximability for higher modes in vibration analysis, and possibly explains the fragility of higher-order finite element methods in nonlinear and dynamic applications in which higher modes necessarily participate. In contrast, the entire NURBS spectrum converges for all modes. This dramatic result is all the more compelling when we recall that the result is independent of the geometry in this one-dimensional setting. Results such as these can be understood from a more fundamental functional analysis perspective through the notion of Kolmogorov n-widths.

6. Kolmogorov n-widths

The approximation result (34) is a basic tool for proving convergence of NURBS to the solution of partial differential equations with h-refined meshes (see [3] for examples). Note that the continuity of the basis functions does not explicitly appear in (34). Consequently, the order of convergence in (34) depends only on the order of the basis functions employed. However, the results of eigenvalue calculations indicate that there is a dramatic difference between C^0- and C^{p-1}-continuous p^{th}-order basis functions (see, $e.g.$, Figure 6). In Figure 6, as p is increased, the upper part of the spectrum $diverges$ for C^0-continuous classical finite elements whereas it $converges$ for C^{p-1}-continuous NURBS ($i.e.$, B-splines in this case). This phenomenon is not revealed by standard approximation theory results of the form (34). Consequently, we much conclude that there is a lot of information hiding in the so-called "constant" C in (34). Indeed, the refined approximation result (35) illustrates an explicit dependence

of the constant on polynomial order *and* continuity. However, the result is quite limited in its application as it is restricted to C^{k-1} approximations, with $2k - 1 \leq p$.

It would be desirable to develop a mathematical framework that revealed behavior like that seen in Figures 6 from the outset. The concept of Kolmogorov n-widths seems to hold the potential to do so. A sketch of some of the main ideas follows: Let X be a normed, linear space, equipped with norm $\|\cdot\|_X$. In the cases of primary interest here, X would be a Sobolev space. Let X_n be an n-dimensional subspace of X. Assume we wish to approximate a given $x \in A \subset X$, where A is a subset of X, with a member $x_n \in X_n$. We define the **distance** between x and X_n as

$$E(x, X_n; X) = \inf_{x_n \in X_n} \|x - x_n\|_X, \tag{52}$$

where inf stands for infimum (see Figure 7). If there exists an x_n^* such that

$$\|x - x_n^*\|_X = E(x, X_n; X) \tag{53}$$

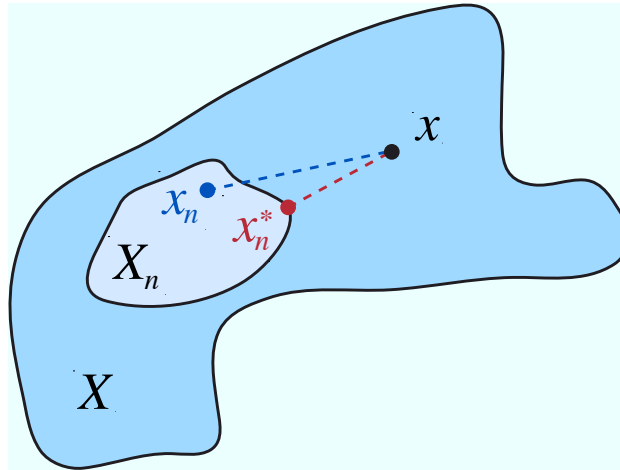then x_n^* is called the **best approximation** of x.

Figure 7. The point x_n^* is the closest approximation in X_n to x with respect to the norm $\|\cdot\|_X$.

Now we assume we are interested in approximating all $x \in A$. For each $x \in A$, the best we can do is expressed by (53). The question we wish to have answered is, for which $x \in A$ do we get the *worst* best-approximation? In other words, for which $x \in A$ is $\inf_{x_n \in X_n} \|x - x_n\|_X$ the largest? The idea is to anticipate situations such as those depicted in Figures 6. The worst best-approximation is obtained by computing the supremum of (53) over all $x \in A$;
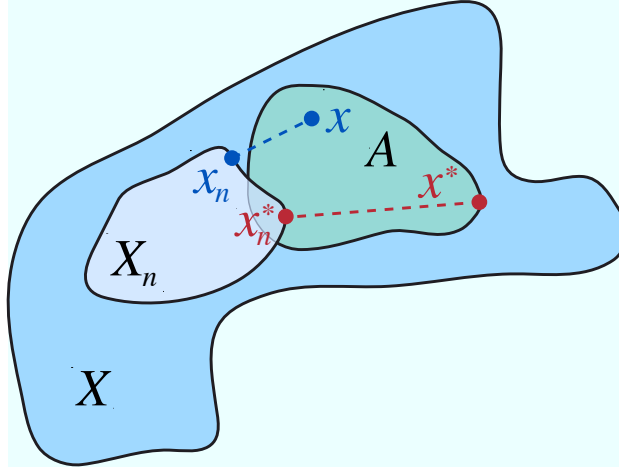
Figure 8. The distance between subspaces X_n and A is determined by the "worst-case scenario." That is, if the distance between point $x^* \in A$ and its best approximation $x_n^* \in X_n$ is the supremum over all such best-fit pairs, then $\|x^* - x_n^*\|_X$ defines the distance between X_n and A.

we define the ***deviation***, or "sup-inf," as

$$E(A, X_n; X) = \sup_{x \in A} \inf_{x_n \in X_n} \|x - x_n\|_X. \tag{54}$$

See Figure 8 for a schematic illustration. Sup-inf's are useful for comparing the approximation quality of different finite element subspaces, such as C^0 and C^{p-1} splines, but prior to that we might ask what is the best n-dimensional subspace for approximating A? This is given by the ***Kolmogorov n-width***, or "inf-sup-inf," namely,

$$d_n(A, X) = \inf_{\substack{X_n \subset X \\ \dim X_n = n}} \sup_{x \in A} \inf_{x_n \in X_n} \|x - x_n\|_X \tag{55}$$

$$= \inf_{\substack{X_n \subset X \\ \dim X_n = n}} E(A, X_n; X). \tag{56}$$

If there exists an $\tilde{X}_n$ such that

$$E(A, \tilde{X}_n; X) = d_n(A, X), \tag{57}$$

then $\tilde{X}_n$ is called an ***optimal n-dimensional subspace***. In this case, we can define the ***optimality ratio***, that is, the sup-inf divided by the inf-sup-inf, for a given X_n:

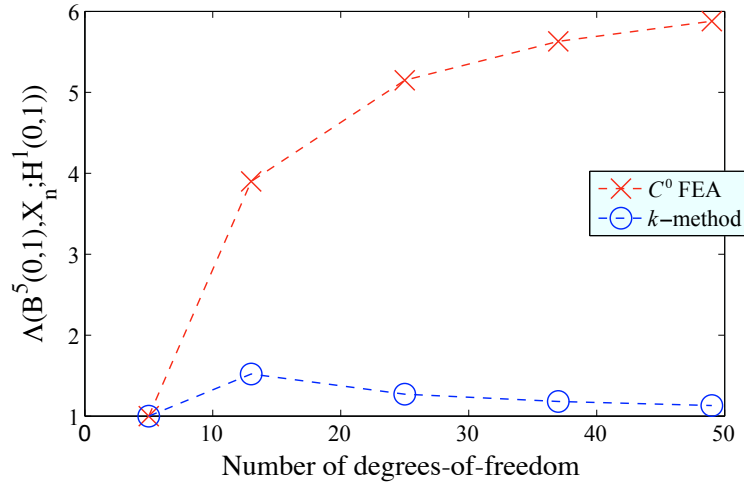$$\Lambda(A, X_n; X) = \frac{E(A, X_n; X)}{d_n(A, X)}. \tag{58}$$

Figure 9. The optimality ratio for approximating the H^5 unit ball in H^1 using quartic ($p = 4$) elements. As the number of degrees-of-freedom increases, the optimality ratio of C^0 FEA functions diverges, while the optimality ratio of C^3-continuous splines converges toward 1.

To illustrate how one might use this measure for comparing spaces, consider the following example of a uniform mesh on the unit interval $[0,1]$. Let $X = H^1(0,1)$, the Sobolev space of square-integrable functions with square-integrable derivatives. Let

$$A = B^5(0,1) = \{x|x \in H^5(0,1), \|x\|_X \leq 1\}, \tag{59}$$

where $H^5(0,1)$ is the Sobolev space of functions having five square-integrable derivatives. $B^5(0,1)$ is referred to as the unit ball in $H^5(0,1)$ in the $H^1(0,1)$-topology. A comparison of optimality ratios for quartic C^0 and C^3 splines is shown in Figure 9. Note that as n increases, the optimality ratio of the C^3 case approaches 1. Apparently, the C^3 case is converging toward an optimal subspace. In contrast, in the C^0 case, the optimality ratio converges to approximately 5.5, indicating that for each n there is at least one member of $B^5(0,1)$ that is much more poorly approximated by C^0 splines than C^3 splines. This result seems to be qualitatively consistent with what we saw in Figures 6. Smooth spline bases, that is the k-method, exhibit better behavior than classical C^0 elements. For further results and methodology used to compute them, see [16].

7. Smooth Isogeometric Discretizations

From the mathematical side, one of the most interesting aspects of Isogeometric Analysis is the possibility to have smooth approximation fields. Smooth discrete

spaces can be directly used with partial differential equations of order higher than two. One interesting example is the stream-function approach to the Stokes problem (see [1]). The solution of the Stokes variational equations is the pair[5] $(\mathbf{u}, p) \in (H_D^1(\Omega))^2 \times L^2(\Omega)$ such that

$$
\begin{cases}
\displaystyle\int_\Omega \mathbf{grad}\,(\mathbf{u}) : \mathbf{grad}\,(\mathbf{v}) + \int_\Omega p\,\mathrm{div}\,\mathbf{v} = \int_\Omega \mathbf{f}\cdot\mathbf{v} & \forall \mathbf{v} \in H_D^1(\Omega) \\[2ex]
\displaystyle\int_\Omega q\,\mathrm{div}\,\mathbf{u} = 0 & \forall q \in L^2(\Omega),
\end{cases}
\tag{60}
$$

where $H_D^1(\Omega)$ is the Sobolev space of H^1 functions vanishing on $\Gamma_D \subset \partial\Omega$. For two-dimensional problems, the divergence-free field $\mathbf{u}$ can be represented as the **curl** of a potential, the so called *stream function*, that is $\mathbf{u} = \mathbf{curl}\,\psi$. Since $\mathrm{div}\,(\mathbf{curl}\,\psi) = 0$, one can replace (60) with

$$
\int_\Omega \mathbf{grad}\,(\mathbf{curl}\,\psi) : \mathbf{grad}\,(\mathbf{curl}\,\phi) = \int_\Omega \mathbf{f}\cdot\mathbf{curl}\,\phi \qquad \forall\phi \in H^2(\Omega)
\tag{61}
$$
$$
+ \text{ boundary conditions.}
$$

The advantage of the above formulation is that at the discrete level, replacing $H^2(\Omega)$ with a suitable NURBS space with at least global C^1-continuity, one obtains an approximation $u_h = \mathbf{curl}\,\psi_h$ which is exactly divergence-free.

The application of this approach to a more realistic problem is presented in [2] where the capability of various numerical methods to correctly reproduce the stability range of finite strain (nonlinear) problems in the incompressible regime is studied. The stream-function isogeometric NURBS approach is applied to a linearized problem at each Newton step of the finite strain problem. This technique is able to sharply estimate the stability limits of the continuous problem in contrast with various standard finite element methods. For example, a simple benchmark problem (an elastic incompressible square in plain strain under constant body load and clamped on three sides) is shown to be stable under compression up to a loading factor of 6.6, while various finite element methods show instabilities around a loading factor of 1.

Another application area where smooth isogeometric discretizations can be utilized is the numerical simulation of phase-field models. Phase-field models provide an alternative description for phase-transition phenomena. The key idea in the phase-field approach is to replace sharp interfaces by thin transition regions where the interfacial forces are smoothly distributed. The transition regions are part of the solution of the governing equations and, thus, front tracking is avoided. Phase-field models are typically characterized by higher-order differential operators and hence require smooth discretization techniques. Isogeometric Analysis has been applied to several phase-field models, including the Cahn-Hilliard equation [18] and the Navier-Stokes-Korteweg equations [19].

---

[5]Here p is the *pressure* instead of the degree.

8. Vector Field Discretizations

An alternate approach to stream-functions which can also handle problems with a solenoidal constraint is the construction of B-splines or NURBS spaces which fulfill the divergence-free property exactly. This is possible once again due to the smoothness of isogeometric spaces, leading to an extension of classical Raviart-Thomas elements. These new discretizations can be used for a much wider class of problems (*e.g.*, Stokes flow (60)) than classical Raviart-Thomas elements. In [9], smooth Raviart-Thomas B-splines and NURBS spaces are introduced and their study is initiated. In [7], these spaces are used in the simulation of incompressible fluid flows.

The mathematical structure behind the construction in [9] can be understood in the framework of the Exterior Calculus. This has been done in [8] where a De Rham complex for B-spline spaces[6] is constructed. Notably, there exist B-spline spaces X_h^i, $i = 0, \ldots, 3$, of any degree and commuting projectors Π^i, $i = 0, \ldots, 3$ such that

$$
\begin{array}{ccccccc}
H^1(\Omega) & \xrightarrow{\ \mathbf{grad}\ } & \mathbf{H}(\mathbf{curl};\Omega) & \xrightarrow{\ \mathbf{curl}\ } & \mathbf{H}(\mathrm{div};\Omega) & \xrightarrow{\ \mathrm{div}\ } & L^2(\Omega) \\
\Pi^0 \downarrow & & \Pi^1 \downarrow & & \Pi^2 \downarrow & & \Pi^3 \downarrow \\
X_h^0 & \xrightarrow{\ \mathbf{grad}\ } & X_h^1 & \xrightarrow{\ \mathbf{curl}\ } & X_h^2 & \xrightarrow{\ \mathrm{div}\ } & X_h^3.
\end{array}
\tag{62}
$$

The above diagram paves the way to stable discretizations of a wide class of differential problems. For example, it provides *spurious free* smooth approximation of the Maxwell eigenproblem: find $\omega \in \mathbb{R}$, and $\mathbf{u} \in \mathbf{H}(\mathbf{curl};\Omega)$, $\mathbf{u} \neq \mathbf{0}$ such that

$$
\int_\Omega \mathbf{curl}\,\mathbf{u} \cdot \mathbf{curl}\,\mathbf{v} = \omega^2 \int_\Omega \mathbf{u} \cdot \mathbf{v} \quad \forall \mathbf{v} \in \mathbf{H}(\mathbf{curl};\Omega).
\tag{63}
$$

For more details, see [8].

9. Conclusions

We have presented a brief mathematical introduction to Isogeometric Analysis, a new numerical methodology for solving partial differential equations (PDEs) that combines and synthesizes Computer Aided Design (CAD) and Finite Element Analysis (FEA) technologies. A main motivation of Isogeometric Analysis is to simplify the process of building FEA models from CAD files, a major bottleneck in the overall engineering process. However, Isogeometric Analysis has also provided new insights and methods for solving PDEs. By way of an

---

[6]Note that these are B-splines and not NURBS.

example, we have shown that Isogeometric Analysis can provide more accurate solutions of PDEs than classical C^0-continuous finite elements. However, these differences are not revealed by standard error analysis procedures utilizing functional analysis techniques in that they are rather insidiously hidden in "constants" in functional analysis inequalities. The example also illustrates a striking deficiency of classical, higher-order, C^0-continuous finite elements, namely, the errors in higher modes diverge with increasing polynomial order. This surprising result seems to explain the observed fragility of these finite element spaces when used to obtain the solution of nonlinear problems, which often involve higher-mode behavior. We also reported on initial investigations using Kolmogorov n-widths to computationally determine the relative merits of finite-dimensional approximating spaces. This amounts to an *a priori* approach capable of exposing deficiencies of approximating spaces for computing the solutions of PDEs.

We have also noted that the smooth, higher-order basis functions of Isogeometric Analysis open the way to efficiently solving higher-order PDEs on complex domains. Problems of this kind, such as those representing multi-phase phenomena, have proven very difficult for standard FEA approaches. Finally, we briefly reviewed recent mathematical work in Isogeometric Analysis devoted to the construction of smooth, divergence-free, approximating spaces for vector field problems, and mentioned seminal functional analysis results that explicitly reveal the improvements garnered by the smooth approximating spaces used in Isogeometric Analysis.

Acknowledgements

References

[1] F. Auricchio, L. Beirão de Veiga, A. Buffa, C. Lovadina, and A. Reali, *A fully "locking-free" isogeometric approach for plane elasticity problems: A stream-function formulation*, Computer Methods in Applied Mechanics and Engineering, 197, (2007) 160–172.

[2] F. Auricchio, L. Beirão de Veiga, C. Lovadina, and A. Reali, *The importance of the exact satisfaction of the incompressibility constraint in nonlinear elastic-*

ity: Mixed FEMs versus NURBS-based approximations, Computer Methods in Applied Mechanics and Engineering, 199, (2010) 314–323.

[3] Y. Bazilevs, L. Beirão de Veiga, J.A. Cottrell, T.J.R. Hughes, and G. Sangalli, *Isogeometric analysis: approximation, stability, and error estimates for h-refined meshes*, Mathematical Models and Methods in Applied Sciences, 16, (2006) 1031–1090.

[4] Y. Bazilevs, V.M. Calo, J.A. Cottrell, J.A. Evans, T.J.R. Hughes, S. Lipton, M.A. Scott, and T.W. Sederberg, *Isogeometric analysis using T-splines*, Computer Methods in Applied Mechanics and Engineering, 199, (2010) 229–263.

[5] Y. Bazilevs, V.M. Calo, Y. Zhang, and T.J.R. Hughes, *Isogeometric fluid-structure interaction analysis with applications to arterial blood flow*, Computational Mechanics, 38, (2006) 310–322.

[6] L. Beirão da Veiga, A. Buffa, J. Rivas, and G. Sangalli, *Some estimates for h-p-k-refinement in isogeometric analysis*, Technical report, IMATI-CNR Preprint, 2009.

[7] A. Buffa, C. De Falco, and G. Sangalli, *Isogeometric analysis: New stable elements for the Stokes equation*, Technical Report, IMATI-CNR Preprint, 2010.

[8] A. Buffa, J. Rivas G. Sangalli, and R. Vázquez, *Isogeometric analysis in electromagnetics: Theory and Testing*, Technical Report, IMATI-CNR Preprint, 2010.

[9] A. Buffa, G. Sangalli, and R. Vázquez, *Isogeometric analysis in electromagnetics: B-splines approximation*, Computer Methods in Applied Mechanics and Engineering, 199, (2010) 1143–1152.

[10] P.G. Ciarlet, *The Finite Element Method for Elliptic Problems*, North-Holland, 1978.

[11] E. Cohen, R.F. Reisenfeld, and F. Elber, *Geometric Modeling with Splines: An Introduction*, A.K. Peters, Ltd., 2001.

[12] J.A. Cottrell, T.J.R. Hughes. and Y. Bazilevs, *Isogeometric Analysis: Toward Integration of CAD and FEA*, Wiley, 2009.

[13] J.A. Cottrell, T.J.R. Hughes, and A. Reali, *Studies of refinement and continuity in isogeometric analysis*, Computer Methods in Applied Mechanics and Engineering, 196, (2007) 4160–4183.

[14] J.A. Cottrell, A. Reali, Y. Bazilevs, and T.J.R. Hughes, *Isogeometric analysis of structural vibrations*, Computer Methods in Applied Mechanics and Engineering, 195, (2006) 5257–5296.

[15] M.R. Dorfel, B. Juttler, and B. Simeon, *Adaptive isogeometric analysis by local h-refinement with T-splines*, Computer Methods in Applied Mechanics and Engineering, 199, (2010) 264–275.

[16] J.A. Evans, Y. Bazilevs, I. Babuška, and T.J.R. Hughes, *n-widths, sup-infs, and optimality ratios for the k-version of the isogeometric finite element method*, Computer Methods in Applied Mechanics and Engineering, 198, (2009) 1726–1741.

[17] G.E. Farin, *NURBS Curves and Surfaces: From Projective Geometry to Practical Use*, A.K. Peters, Ltd., 1999.

[18] H. Gomez, V.M. Calo, Y. Bazilevs, and T.J.R. Hughes, *Isogeometric analysis of the Cahn-Hilliard phase-field model*, Computer Methods in Applied Mechanics and Engineering, 197, (2008) 4333–4352.

[19] H. Gomez, T.J.R. Hughes, X. Noguerira, and V.M. Calo, *Isogeometric analysis of the isothermal Navier-Stokes-Korteweg equations*, Computer Methods in Applied Mechanics and Engineering, 199, (2010) 1828–1840.

[20] T.J.R. Hughes, *The Finite Element Method: Linear Static and Dynamic Finite Element Analysis*, Dover, 2000.

[21] T.J.R. Hughes, J.A. Cottrell, and Y. Bazilevs, *Isogeometric analysis: CAD, finite elements, NURBS, exact geometry and mesh refinement*, Computer Methods in Applied Mechanics and Engineering, 194, (2005) 4135–4195.

[22] L. Piegl and W. Tiller, *The NURBS Book (Monographs in Visual Communication), Second Edition*, Springer-Verlag, 1997.

[23] D.F. Rogers, *An Introduction to NURBS with Historical Perspective*, Academic Press, 2001.

[24] T.W. Sederberg, D.L. Cardon, G.T. Finnigan, N.S. North, J.M. Zheng, and T. Lyche, *T-spline simplication and local refinement*, ACM Transactions on Graphics, 23, (2004) 276–283.

[25] T.W. Sederberg, J.M. Zheng, A. Bakenov, and A. Nasri, *T-splines and T-NURCCSs*, ACM Transactions on Graphics, 22, (2003) 477–484.

[26] G. Strang and G.J. Fix, *An Analysis of the Finite Element Method*, Prentice-Hall, 1973.

[27] T-Splines, Inc. http://www.tsplines.com/maya/ (2010).

[28] T-Splines, Inc. http://www.tsplines.com/rhino/ (2010).